ELSEVIER

Journal of Applied Geophysics 45 (2000) 49–61

JOURNAL OF APPLIED GEOPHYSICS

www.elsevier.nl/locate/jappgeo

Application of the Hartley transform for interpretation of gravity anomalies in the Shamakhy–Gobustan and Absheron oil- and gas-bearing regions, Azerbaijan

Fakhraddin A. Kadirov *

Department of Geophysics, Institute of Geology, Azerbaijan Academy of Sciences, H. Cavid pr., 29A, Baku, Azerbaijan
Department of Geophysical Engineering, Black Sea Technical University, 61080 Trabzon, Turkey

Received 21 July 1999; accepted 14 April 2000

Abstract

Gravity data acquired in the Shamakhy–Gobustan and Absheron oil- and gas-bearing regions were filtered using a Hartley transform (HT) and Butterworth filter. The HT, originally introduced by Hartley [Hartley, R.V.L., 1942. A more symmetrical Fourier analysis applied to transmission problems. Proc. IRE, 30(2), pp. 144–150], is an integral transform method similar to the Fourier transform (FT) with a number of properties being similar to the properties of FT. The HT is a real transform. It is an alternative procedure to the discrete FT since one complex operation is equal to four real operations. The experiments show that the discrete HT is twice as fast as the discrete FT. The power spectrum of the HT analysis of the Bouguer gravity values in the Shamakhy–Gobustan and Absheron regions suggests that a gravity field may be separated into long- and short-wavelength components. The power spectrum indicates a depth of 24.5 km for the long component and 3.2 km for the short one. No relationship has been revealed between the gravity anomalies and the surface tectonics. The regional anomalies are interpreted to be related with elevation and the sinking of the crystalline basement.

Keywords: Gravity anomaly; Hartley transform; Power spectrum; Filtering; Oil and gas fields; Absheron peninsula

1. Introduction

Tsimmelzon (1965) and Gadjiyev (1965) studied and interpreted the gravity anomalies of the area using elliptic and quadratic pallets. In this work, a Hartley transform (HT) (Hartley, 1942) has been utilized to determine local and regional gravity anomalies of the Absheron and Shamakhy–Gobustan oil and gas fields. There are similarities between HTs and Fourier transforms (FTs), however, the former is faster and requires less computer memory (Bracewell, 1983; Saatcilar et al., 1990).

The study area is located in the southeast side of the Great Caucasus mega-anticlinorium. The region has specific geologic structures and tectonics. Fig. 1 gives the tectonic and geological scheme of the area (Agabekov et al., 1972). In

* Department of Geophysics, Institute of Geology, Azerbaijan Academy of Sciences, H. Cavid pr., 29A, Baku, Azerbaijan. Fax: +7-99412-97-52-83, +7-99412-97-52-85.
E-mail address: gia@azeurotel.com (F.A. Kadirov).

0926-9851/00/$ - see front matter
PII: S0926-9851(00)00018-5

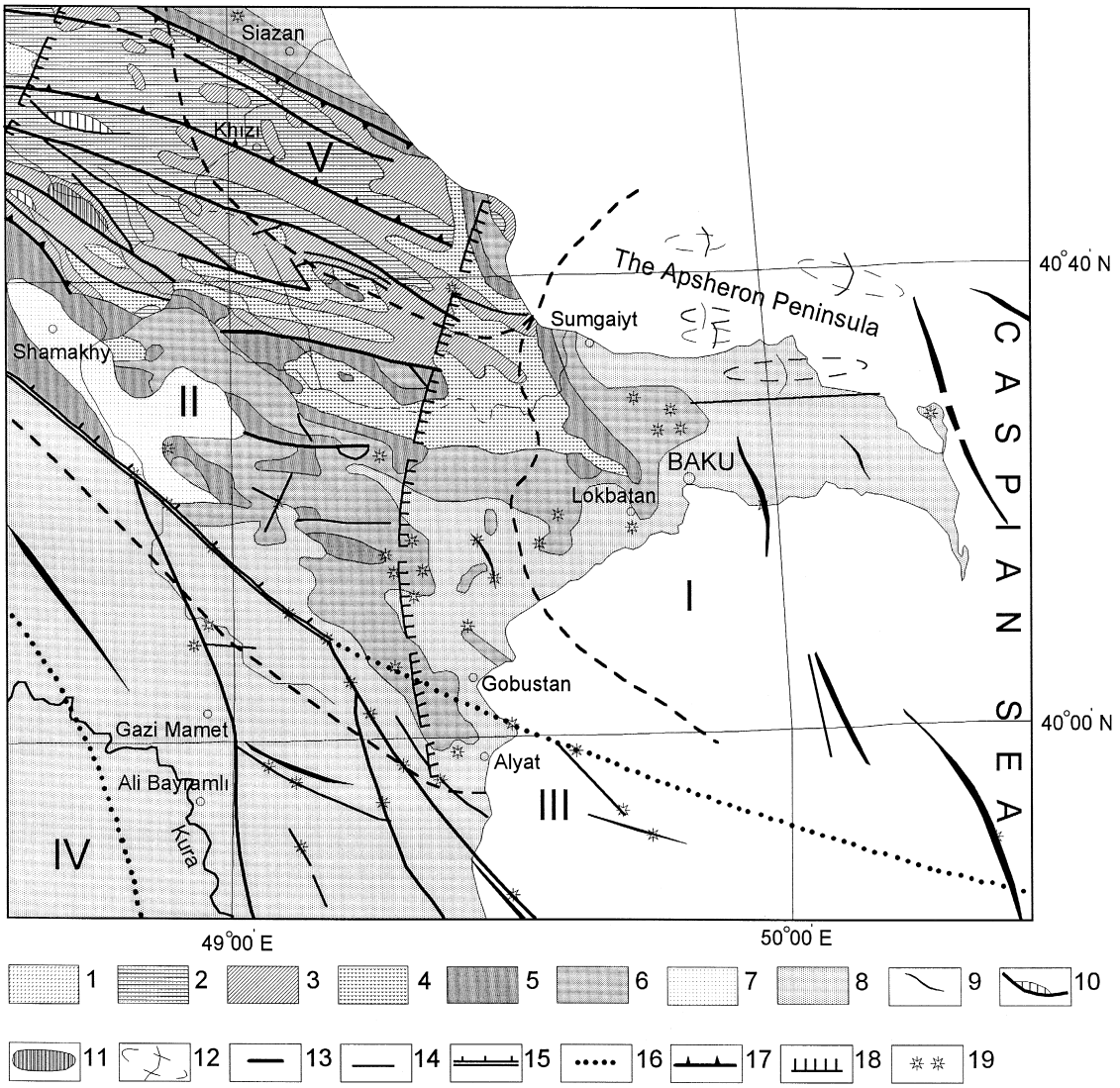

Fig. 1. Tectonic and geological scheme of the study area. Alpine geosynclinal sub-complexes: 1 — early geosynclinal epoch ($g_1 AJ_{1-2}$), late geosynclinal epoch: 2 — lower epoch ($g_2^1 AJ_3 - K_1 ap$), 3 — middle epoch ($g_2^2 AK_1 al - K_2$), 4 — upper epoch ($g_2^3 AP_{1-2}$). Alpine orogenesis sub-complexes: 5 — early orogenesis sub-epoch ($o_1^1 AP_3 - N_1^1$), 6 — early orogenesis upper epoch ($o_1^2 AN_1^2 - N_2^2$), 7 — late orogenic epoch up to 800 m ($o_2 AN_2^3 - Q$), 8 — late orogenic epoch 800 m and greater (O_2). Structural elements, fold types and dislocations with a break in continuity: 9 — axes of large anticlinal folds, 10 — scale-shaped folds, 11 — tectonic nappe, 12 — buried folds, 13 — normal faults with thousands of meters of amplitude, 14 — normal faults with hundreds of meters of amplitude, 15 — crustal faults manifested at the surface by thrusts and overfaults, 16 — buried faults, 17 — thrusts and overfaults with thousands of meters of amplitude, 18 — buried flexure, 19 — mud volcano. Oil- and gas-bearing regions: I — Absheron region, II — Shamakhy–Gobustan region, III — Baku Archipelago, IV — Lower Kura region, V — near-Caspian region.

the region, mud-volcanic and diapir folds are widespread. The Tengi–Beshbarmag anticlinorium, Shahdag–Khyzy, Zakatala–Govdag, Shamakhy–Gobustan synclinoria, Absheron and the Lower Kura basins are the main tectonic structural elements (Shikhalibeyli, 1972). The area embraces the whole of the Absheron oil- and gas-bearing region, a large part of the

Shamakhy–Gobustan region, some parts of the Baku Archipelago, the Lower Kura and near-Caspian oil- and gas-bearing regions. Intensive subsidence in the Shamakhy–Gobustan synclinorium began in the Cretaceous and Paleogene periods. The great thicknesses of the Paleogene–Neogene deposits and the clearly expressed boundaries of their occurrence, represented in the west by Zangi and in the east by Goradil thrusts, lend support to this subsidence.

A comparison of geological and geophysical data from the Shamakhy–Gobustan synclinorium indicates that the structural features of the Mesozoic and Cenozoic strata are discordant. The synclinorium is considered as a superimposed trough of complicated structure. Its southwest boundary is made up of the Lengebiz–Alyat anticline zone. The present structure of the Lengebiz–Alyat zone was formed in the late Pliocene–Quaternary period. The Absheron periclinal trough is superimposed in character and represents an extreme eastern structural element of the Great Caucasus mega-anticlinorium. In the west, the trough is limited by the Yashma flexure, the origin of which is related to the Cenozoic subsidence of the Caspian basin. As a consequence, substantial sinking of the Absheron peninsula and of the North Absheron aquatorium, along with the islands and banks, occurred. Simultaneously, the eastern part of the Shamakhy–Gobustan synclinorium (the Jeyrankechmez depression), composed of Paleogene and Miocene sediments, was involved in this process.

According to borehole and geophysical data, the depth of the Mesozoic top within the study area varies in the range of 1–10 km. In the central part of the Jeyrankechmez depression, the top of the Paleogene–Miocene complex lies below 3–4 km and that of the Mesozoic is within 8–10 km. The Lower Kura basin is the deepest among the basins of the Kura basin system. The major part of the Lower Kura basin is covered with Quaternary strata. The boundaries of the Lower Kura basin are the West Caspian fault and the Lengebiz–Alyat rise in the southwest and northeast, respectively. In the Lower Kura basin, the thickness of the sedimentary pile is around 15 km, of which over 8 km is made up of the Pliocene–Quaternary sediments. The study area is an element of the Alpine-folded belt of Eurasia. The Great Caucasus and the Kura basin experienced tectonic evolution spanning the Late Proterozoic to the Anthropogene period. In general, three periods are differentiated in the geological evolution of Azerbaijan: Baikalian, Hercynian and Alpine. The area along the Great Caucasus axis and its south slope is supposed to belong to the Paleozoic geosyncline (Azizbekov et al., 1972).

2. Gravity data in the study area

Gravity data obtained in Azerbaijan made it possible to compose a gravity map at a scale of 1:500,000. To build the gravity map, a density of 2.67 g/cm^3 was assumed to perform the Bouguer correction. Gravity observation error amounts to $\pm 0.07–0.1$ mGal on land, and $\pm 0.2–0.3$ mGal at sea. Normal gravity is calculated by Helmert's formula. When the Bouguer anomaly was calculated, terrain correction had been done. Fig. 2 shows the Bouguer gravity map of the study area. The gridded square constructed on the basis of the Bouguer gravity data set has 32×32 elements both in the west-to-east and south-to-north directions, with the grid interval taken every 5 km in both directions. The East Azerbaijan negative anomaly (with an extreme value at -140 mGal) covers the Absheron–Gobustan area; this type of anomaly is not characteristic of areas of high topography. The Dubrar relative maximum, stretched along the southeast slope of the Great Caucasus, is located in the northwest part of the area. Another non-extensive relative maximum zone goes in the direction from the Yavany Mt. to the Sangachal locality. The axis of this anomaly is stretched parallel to the direction of the Great Caucasus axis. Some of the local anomalies are overshadowed by the regional

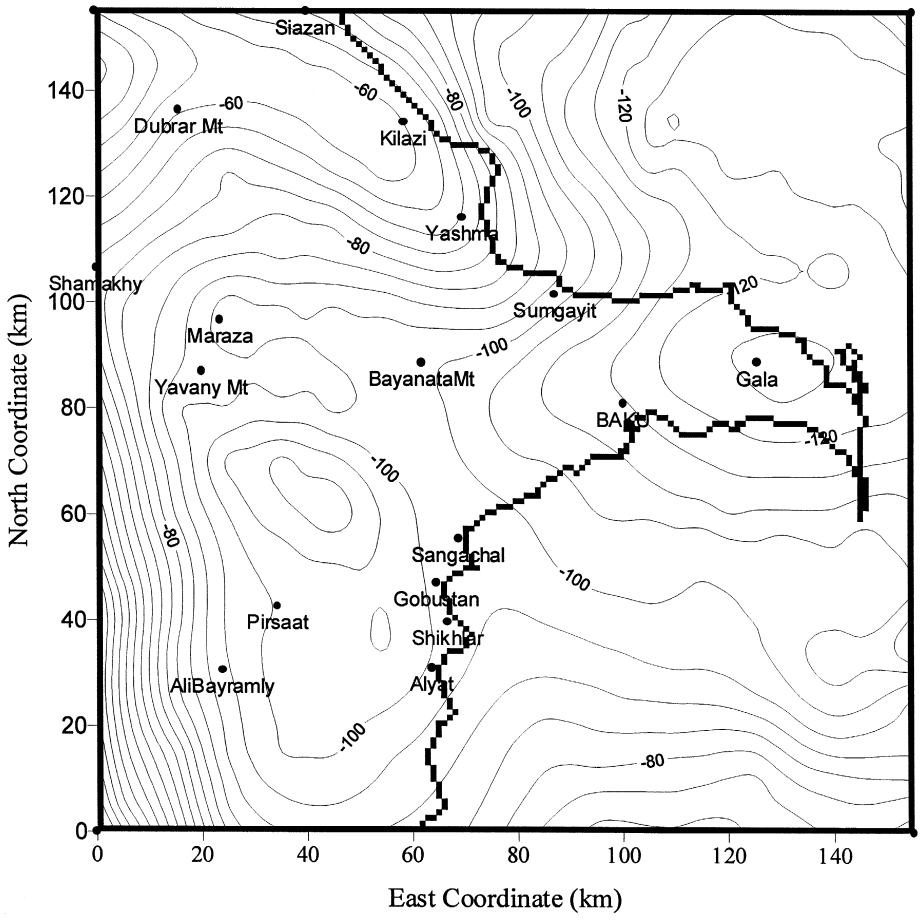

Fig. 2. Bouguer gravity map for the study area. Contour interval is 5 mGal.

anomalies clearly outlined in the map. A comparison of the Bouguer gravity anomalies with the tectonic and geological scheme of the area suggests no relationship between surface tectonics and gravity distribution.

The following are the objectives of the paper:

- application of the HT for spectral analysis of the gravity data on the Shamakhy–Gobustan and Absheron oil- and gas-bearing regions and evaluation of the mean depths of discrete density boundaries;
- separation of the gravity field into its regional and local components using the Butterworth filter;
- revealing the impact of the crystalline basement on the character of the regional anomalies.

3. Theoretical formulation

The 2-D HT of a real function $f(x,y)$ is defined as:

$$H(u,v) = \int_{-\infty}^{\infty}\int_{-\infty}^{\infty} f(x,y)\mathrm{Cas}(ux) \times \mathrm{Cas}(vy)\,\mathrm{d}x\,\mathrm{d}y, \quad (1)$$

where:

$$\mathrm{Cas}(ux)\mathrm{Cas}(vy) = \cos(ux - vy) + \sin(ux + vy).$$

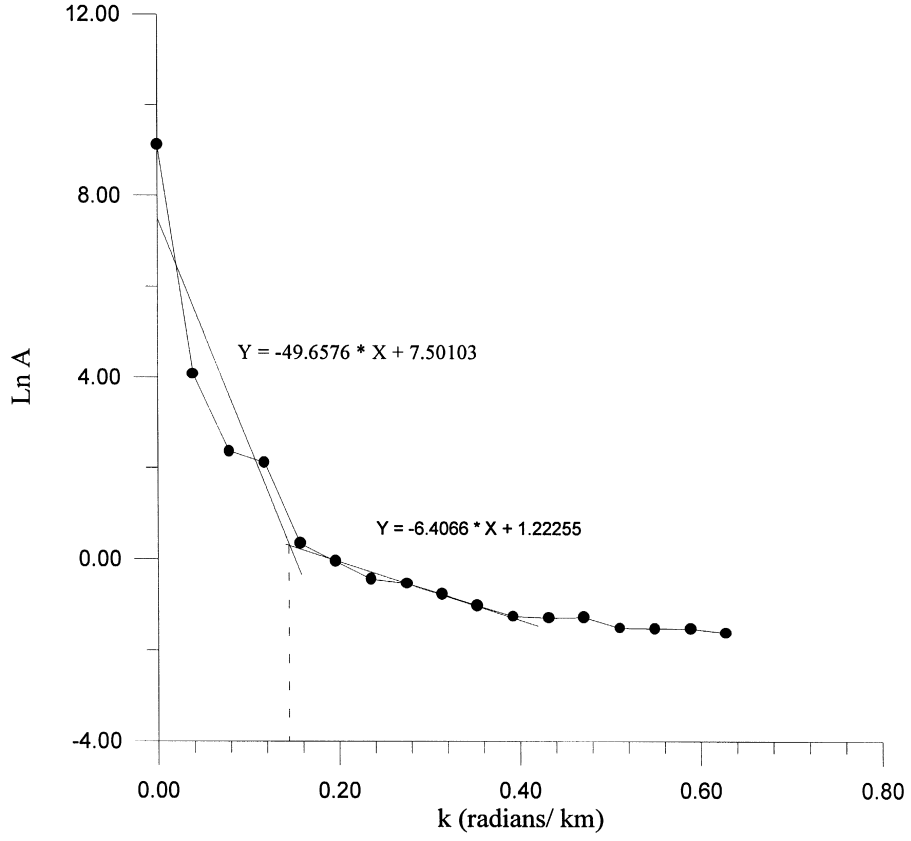

Fig. 3. Power spectrum of the Bouguer gravity anomaly in the study area.

The inverse transform can be obtained by interchanging the positions of $f(x,y)$ and $H(u,v)$ in Eq. (1) and replacing $\mathrm{d}x\mathrm{d}y$ with $\mathrm{d}u\mathrm{d}v$ as below:

$$f(x,y) = \int_{-\infty}^{\infty}\int_{-\infty}^{\infty} H(u,v)\mathrm{Cas}(ux) \times \mathrm{Cas}(vy)\mathrm{d}u\mathrm{d}v. \quad (2)$$

Let $H(u,v) = E(u,v) + O(u,v)$, where $E(u,v)$ and $O(u,v)$ are even and odd functions defined as:

$$E(u,v) = \int_{-\infty}^{\infty}\int_{-\infty}^{\infty} f(x,y)\cos(ux - vy)\mathrm{d}x\mathrm{d}y = \frac{H(u,v) + h(-u,-v)}{2} \quad (3)$$

and:

$$O(u,v) = \int_{-\infty}^{\infty}\int_{-\infty}^{\infty} f(x,y)\sin(ux - vy)\mathrm{d}x\mathrm{d}y = \frac{H(u,v) - H(-u,-v)}{2}, \quad (4)$$

where

$$H(-u,-v) = \int_{-\infty}^{\infty}\int_{-\infty}^{\infty} f(x,y)\mathrm{Cas}(-ux) \times \mathrm{Cas}(-vy)\mathrm{d}x\mathrm{d}y. \quad (5)$$

2-D HTs and FTs are related by (Bracewell, 1986; Mohan and Anand Babu, 1994; Saatcilar et al., 1990):

$$F(u,v) = E(u,v) - iO(u,v), \quad (6)$$

$$H(u,v) = Re\,F(u,v) - Im\,F(u,v), \quad (7)$$

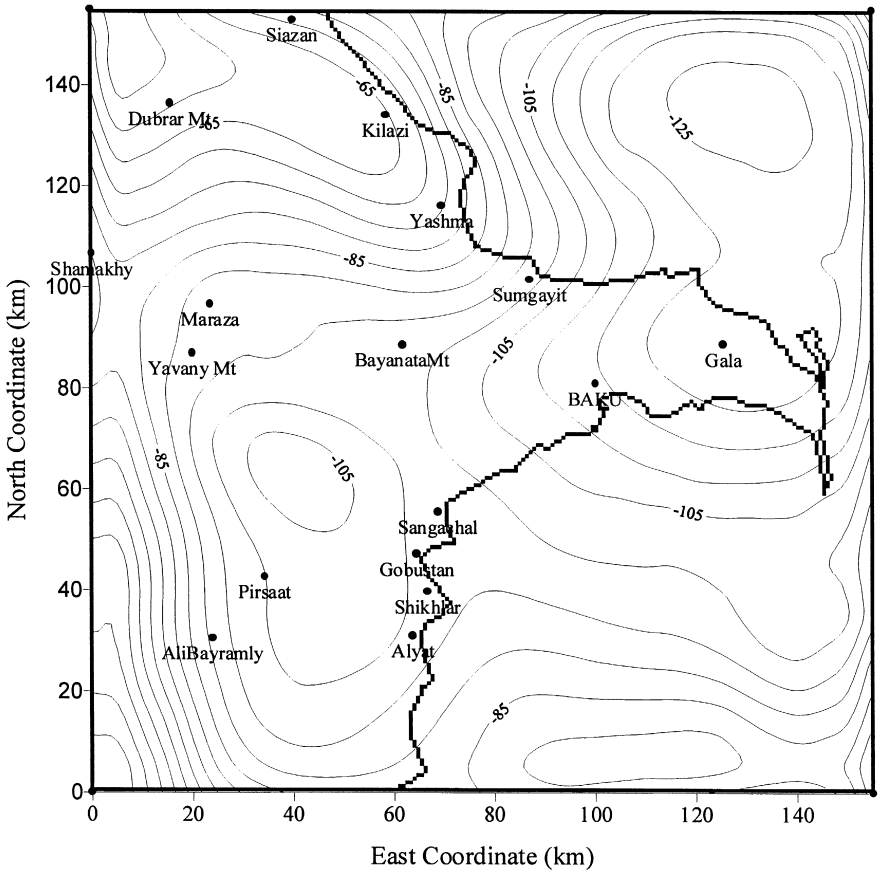

Fig. 4. Results of the low-pass filtering of the gravity data on the study area using 2-D HT.

where $F(u,v)$ is the FT of $f(x,y)$. The amplitude and phase spectra associated with the HT are both physically and mathematically similar to those of the FT but differ numerically. In general, the amplitude spectra of the FT and HT give the same information. The 2-D discrete HT of an image $f(x,y)$ represented by an $(M \times N)$ matrix is defined in accordance with Eq. (1) as below (Sundararajan, 1995):

$$X(u,v) = \frac{1}{MN} \sum_{x=0}^{M-1} \sum_{y=0}^{N-1} f(x,y)\mathrm{Cas}(ux) \times \mathrm{Cas}(vy). \quad (8)$$

Its inverse is given as below:

$$f(x,y) = \sum_{u=0}^{M-1} \sum_{v=0}^{N-1} H(u,v)\mathrm{Cas}(ux)\mathrm{Cas}(vy). \quad (9)$$

The results obtained from Eq. (10) are rearranged to get the 2-D HT by (Rao et al., 1995):

$$H(u,v) = \frac{1}{2}\left[X(u,v) + X(M-u,v) + X(u,N-v) - X(M-u,N-v)\right]$$

for $u \neq 0, v \neq 0$ (10)

and:

$$H(u,v) = X(u,v), \quad \text{for } u = 0 \text{ and } v = 0.$$

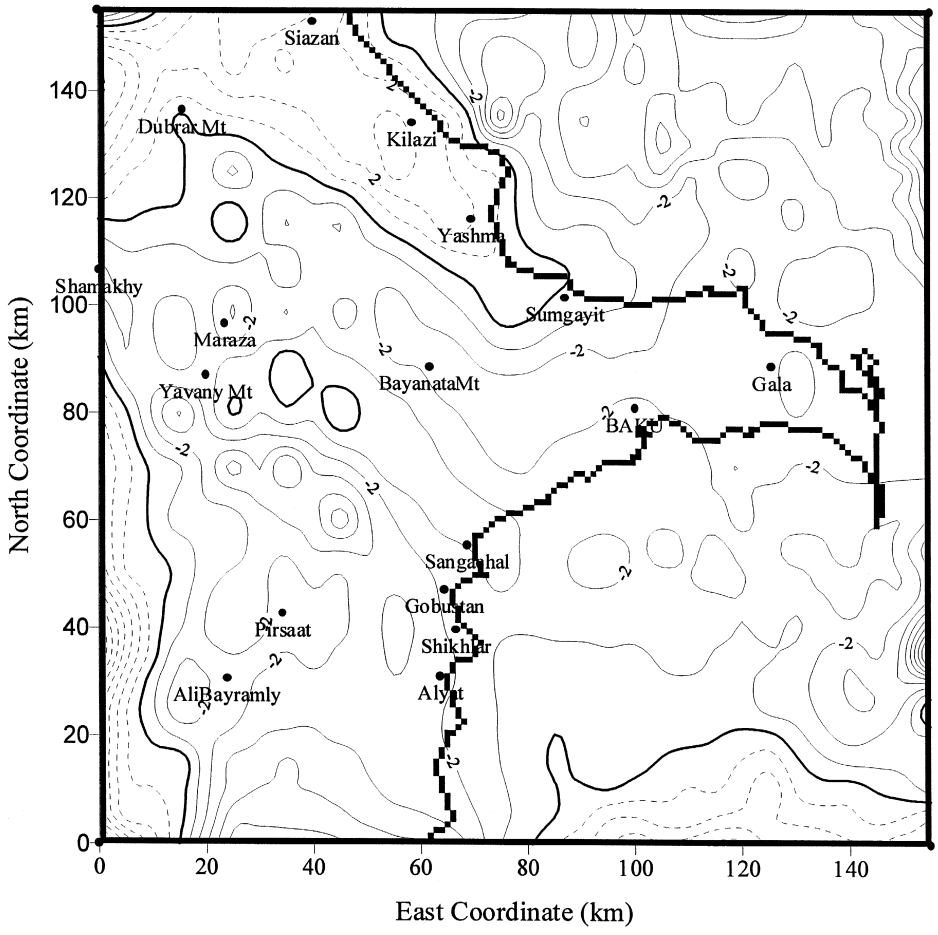

Fig. 5. Results of the high-pass filtering of the gravity data on the study area using 2-D HT. Dashed and solid lines show positive and negative local anomalies, respectively.

The Hartley amplitude coefficients are calculated from positive and negative coefficients as given below:

$$A(u,v) = \left[\frac{H^2(u,v) + H^2(\mathrm{Nu},\mathrm{Mv})}{2} \right]^{1/2} \qquad (11)$$

for Nu and Mv defined as:

$$\begin{aligned} &\mathrm{Nu} = u \\ &\mathrm{Mv} = v \qquad \text{for } u = 0 \text{ and } v = 0, \\ &\mathrm{Nu} = u \\ &\mathrm{Mv} = M - v \qquad \text{for } u = 0 \text{ and } v \neq 0, \\ &\mathrm{Nu} = N - u \\ &\mathrm{Mv} = v \qquad \text{for } u \neq 0 \text{ and } v = 0. \end{aligned} \qquad (12)$$

With these coefficients, even and odd Hartley coefficients can also be calculated.

$$E(u,v) = \frac{H(u,v) + H(\mathrm{Nu},\mathrm{Mv})}{2}$$

and: (13)

$$O(u,v) = \frac{H(u,v) - H(\mathrm{Nu},\mathrm{Mv})}{2}.$$

$E(u,v)$ and $O(u,v)$ are even and odd Hartley coefficients, respectively. The Hartley amplitude and phase spectrum values can be calculated with these coefficients as shown below:

$$A(u,v) = \left[E^2(u,v) + O^2(u,v) \right]^{1/2}$$

$$\Theta(u,v) = \arctan\left[-\frac{O(u,v)}{E(u,v)}\right], \quad (14)$$

where $A(u,v)$ and $\theta(u,v)$ are the amplitude and phase spectra of the HT.

To separate regional and residual anomalies of the Bouguer gravity field, HT and Butterworth filters are used (Kulhânek, 1976). The ideal low-pass Butterworth filter is given by:

$$H_B(k) = \frac{1}{\sqrt{1+\left(\frac{k}{k_c}\right)^{2n}}}, \quad (15)$$

where $k = 2\pi/\lambda$ is the wave number, $k_c = 2\pi/\lambda_c$ is the cut-off wave number and n is the degree of the filter. In this study, n was taken to be equal to 1. The procedure of filtering is: using the HT transform, the gridded gravity data are converted to space-frequency Hartley domain. In this domain, row by row followed by column by column Butterworth filters are applied using a suitable cut-off frequency. Then, the produced filters are multiplied by the spectrum of data in the Hartley domain. Finally, by taking the inverse transform, we return to the space domain.

4. Application to real data

The HT was applied to the gravity data grid of 32×32 dimensions with grid spacing at

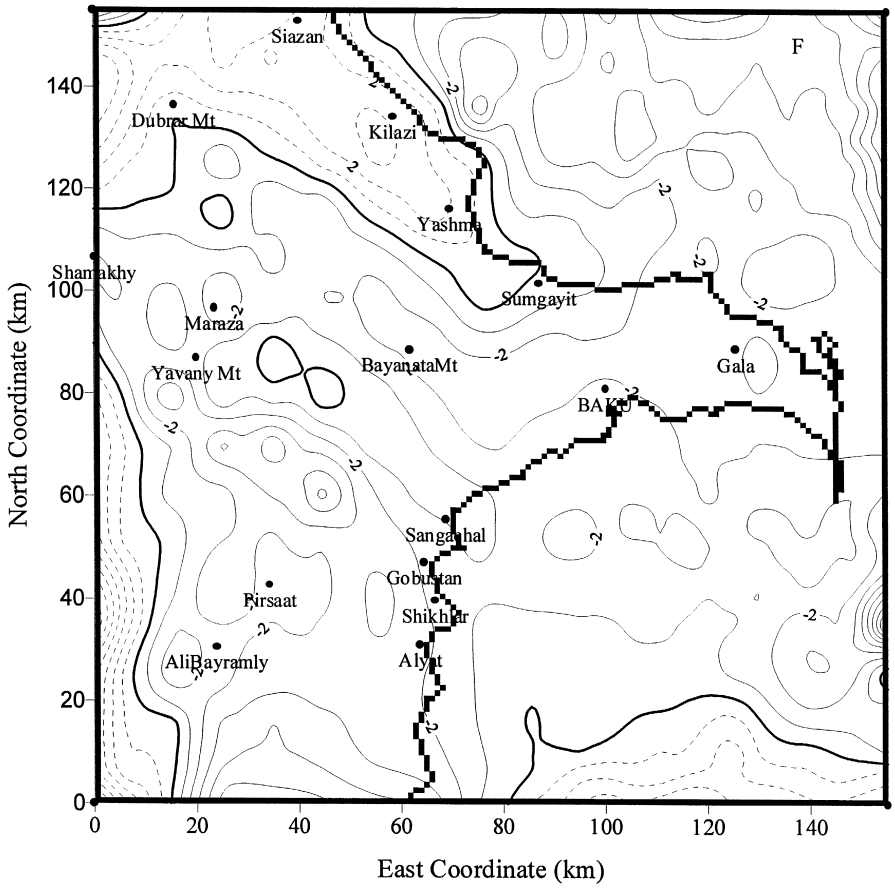

Fig. 6. Results of the high-pass filtering of the gravity data on the study area using 2-D FT. Dashed and solid lines show positive and negative local anomalies, respectively.

every 5 km in the study area. The calculated power spectrum curve is displayed in Fig. 3. The power spectrum of the gravity data shows a cut-off wave number separating two domains of high- and low-wavelength information. The low- and high-wave number parts of the power spectrum, associated with deep and shallow gravity sources, were taken as representing the regional and residual anomalies, respectively. Two linear segments shown on the plot are suggestive of the existence of discrete density boundaries, with the slopes being the estimates of their mean depths (Bhattacharyya, 1966; Spector and Grant, 1970). The present power spectrum indicates a depth of 24.5 km for the long-wavelength component and a depth of 3.2 km for the short wavelength component. These depth values are well-correlated with the results of seismic studies previously carried out in the region.

The cut-off wave number is determined by the crossing point of fitted straight lines approximating the power spectrum data in the high- and low-wavelength domains. A cut-off wave number of $k_c = 0.142$ km^{-1} is found from the power spectrum.

Fig. 4 shows the results of low-pass filtering arranged for a $k_c = 0.142$ km^{-1} wave number. The gravity low north of Absheron is preserved in the regional Bouguer anomaly map. The results of the high-pass filtering process are presented in Fig. 5. A large positive anomaly is evident northwest of the region (from Sumgayit to Siazan), the so-called Dubrar positive anomaly. A maximum local anomaly value of 7 mGal is noted in the Kilazi locality. Another extensive positive anomaly lies parallel to the Great Caucasus axis covering an area from the Yavany Mt. to Sangachal, where the highest value is equal to 3 mGal. In the southwest, a large positive anomaly located within the Kura Plateau is noted. The Absheron–Central Gobustan negative anomaly (as low as -7 mGal) is seen to the east and south of the Dubrar Mt. positive-anomaly region. The Absheron negative anomaly extends towards the north. A row of closed negative anomalies begins from Gobustan and goes towards Shamakhy. The results of the high-pass filtering through the FT are displayed in Fig.6. As can be seen, the contours presented in Figs.5 and 6 are very similar.

5. Model of basement and its gravity effects in the study area

The depth occurrence of the pre-Mesozoic crystalline basement surface has been studied with the aim of interpreting the gravity anomalies in the Absheron and the Shamakhy–Gobustan regions. The density-vs.-depth relationship in the part of the earth's crust overlying

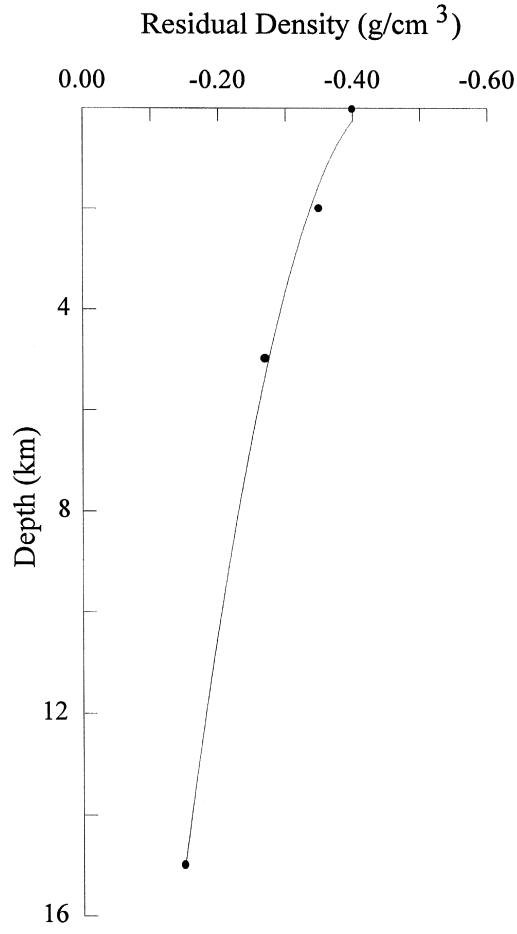

Fig. 7. Approximation of density-vs.-depth data for the study area by a quadratic function.

the crystalline basement can be approximated by a quadratic function (Bhaskara Rao, 1986):

$$\Delta\rho(z) = a_0 + a_1 z + a_2 z^2, \quad (16)$$

where z represents the depth, measured positive in the downward direction, a_0 represents the extrapolated value of the density contrast at the surface, and a_1 and a_2 are the constants of the quadratic function. The constants are first solved by the least squares method on the data of density available from borehole profiles (down to 5 km) and other geophysical information sources.

The geological, geophysical and borehole information available suggest a general four-layer structure of the earth's crust in the area: a first layer of Cenozoic deposits with a density of $\rho = 2.20–2.40$ g/cm^3; a second one of Mesozoic deposits, $\rho = 2.60–2.72$ g/cm^3; a third one of metamorphic and granite rocks, $\rho = 2.66–2.85$ g/cm^3; and the fourth one of basaltic rocks, $\rho = 2.90$ g/cm^3 (Gadjiyev, 1965; Volarovich et al., 1966). The thicknesses of these layers vary substantially over the region, making up around 42 km in total.

In the study area, a considerable density contrast of -0.35 g/cm^3 at a 2-km depth within the Neogene complex is documented by borehole survey. The next density contrast of -0.27 g/cm^3 occurring at the Cenozoic and Mesozoic boundary is located at an average depth of 5 km. At the boundary of the crystalline base-

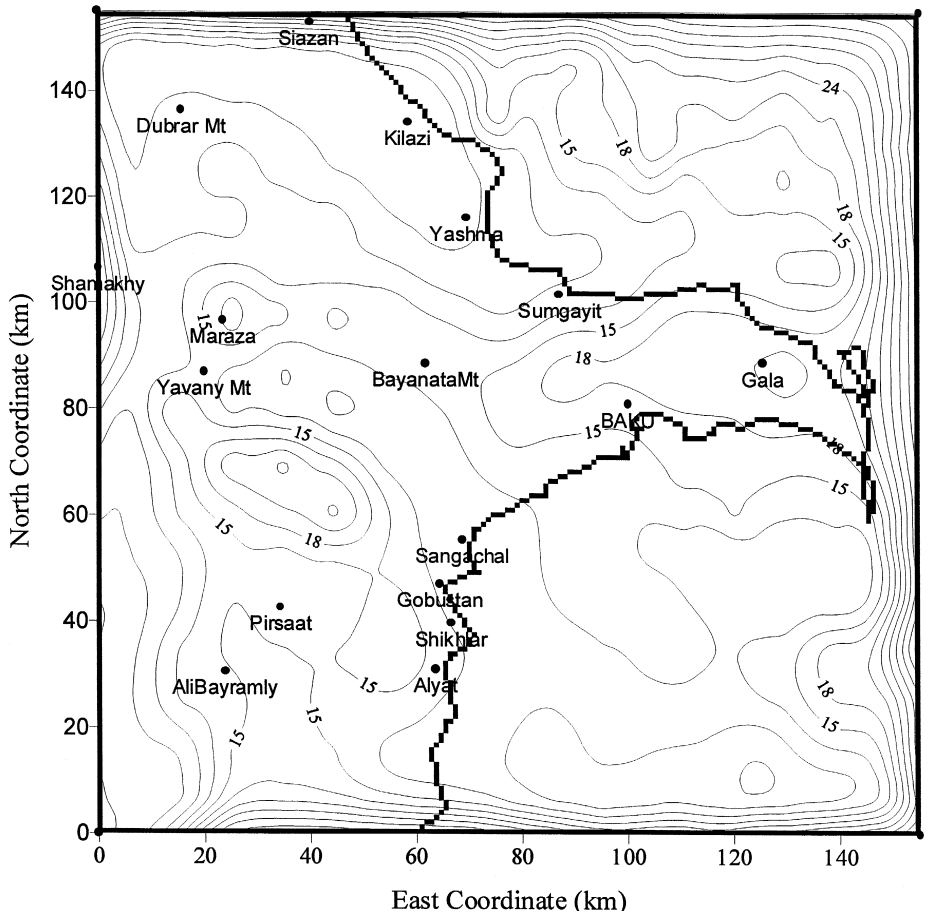

Fig. 8. Basement contour map of the study area derived from 3-D modelling of gravity anomalies using a quadratic density function. Contour interval is 3 km.

ment, occurring at an average depth of 15 km, the density contrast is taken to be equal to $-0.15 g/cm^3$. Besides the layered model is the included density contrast at the boundary of the low-velocity zone (-0.40 g/cm^3).

Taking the mean thicknesses of the Cenozoic and Mesozoic as equal to 5 and 10 km, respectively, with the density contrast between them at -0.27 and -0.15 g/cm^3 at the surface of the crystalline basement, a density-vs.-depth quadratic relationship has been established. The values so obtained are $a_0 = -0.4009$, $a_1 = 0.03091$, and $a_2 = -0.00094$. This approximation function is graphically shown in Fig. 7.

Deep sounding of the subsurface with seismic methods shows that from the north of the Absheron Peninsula to the south, the marine continuation of the Jeirankechmez depression, the thickness of the Pliocene deposits progressively increases. These deposits have the lowest density, being within 2.0–2.2 g/cm^3 on average. Such a north-to-south trend in thickness, with quiescent bedding of the underlying strata, must be accompanied by a decrease of the gravity field in the same direction. At a distance of 50 km, the thickness of the Pliocene unit grows to as large as 7 km. With an average of 0.3-g/cm^3 density difference between the Pliocene and the underlying strata, a 7-km-thick unit must provide a negative gravity field of 89 mGal. However, observed anomalies of the gravity field in the Bouguer reduction in the indicated direction increase. The negative gravity effect due to the Pliocene complex is com-

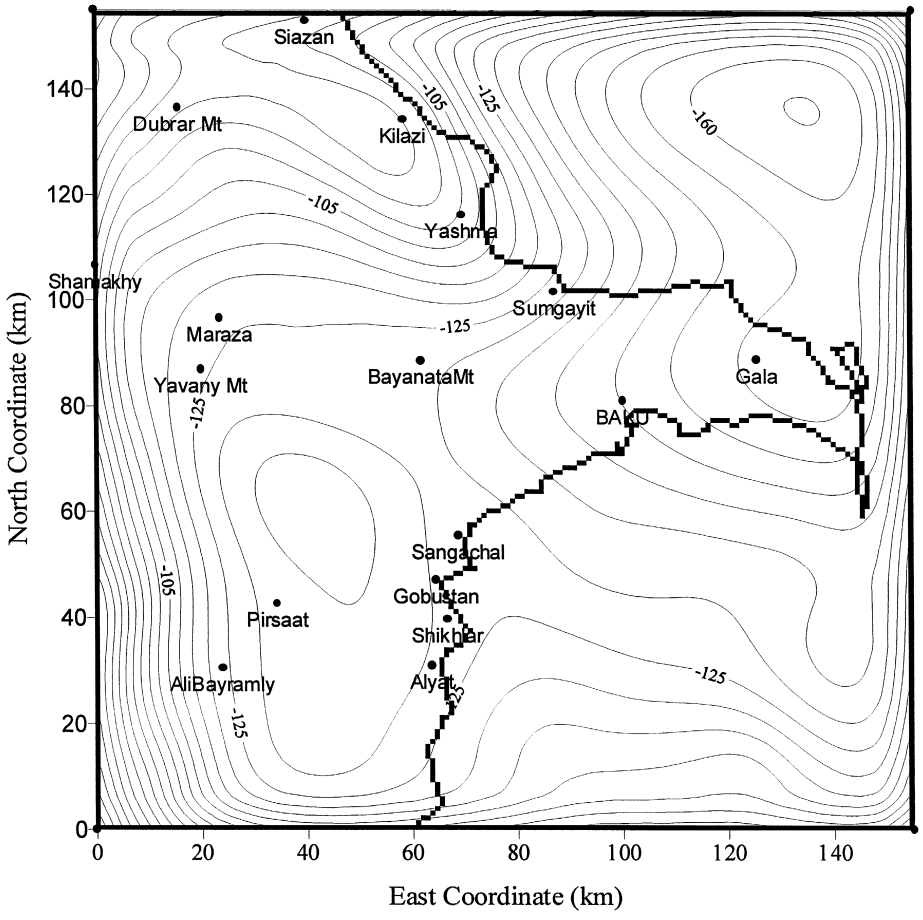

Fig. 9. The calculated gravity anomalies of the sedimentary basin with the 3-D prism program. Contour interval is 5 mGal.

pensated for by a positive gravity effect caused by the southward elevation of the denser rocks (Gadjiyev, 1965). Thus, an increase in the thickness of the young deposits is accompanied by elevation of the denser and older complexes. By subtracting the linear regional effect of 30 mGal due to the elevation of the denser and older rocks from the map of the gravity field anomaly in the Bouguer reduction, we obtain a ''residual'' gravity map of the study area. The depth map of the basement (Fig. 8) is estimated from the inversion of the ''residual'' gravity field constrained with the density model (Fig. 7) by using the GR3DSTR program (Bhaskara and Ramesh, 1991). Calculations for the basement depth maps were performed at specified 10 iterations. The recalculated gravity effect based on the depth-to-basement map (Fig. 8) is displayed in Fig. 9. Apart from the regional shift of 30 mGal, the map agrees well with the regional-anomaly map. As can be seen, higher values on the map correspond to the Yavany Mt.-Alyat area where the mean depth is around 23 km. The mean depths in the Absheron peninsula and the Dubrar zone are 20 and 6 km, respectively. The data presented are well-correlated with the results of seismic exploration (Gadjiyev, 1965; Aksyonovich et al., 1962; Radjabov, 1978). Comparison of the Bouguer-gravity-anomaly maps, regional-anomaly map and calculated gravity anomalies with regard to the above reduction shows that a major part of the regional anomaly is due to the crystalline basement.

6. Conclusions

Using complex numbers is unavoidable when the FT is applied to real geophysical measurements. The real HT does not require operations with complex numbers, being in this way a better alternative to the FT. The results obtained by applying both transforms are in good agreement.

Analysis of the gravity field power spectrum for the Absheron and the Shamakhy–Gobustan regions allows estimation of the average depths of sources varying from 24.5 to 3.2 km. A depth of 24.5 km is associated with the crystalline basement surface, and that of 3.2 km with a surface within the Cenozoic deposits.

The maximum depth of subsidence of the crystalline basement (23 km) is noted in the area of Yavany Mt.–Pirsaat–Gobustan and around Gala. In the zones of Dubrar Mt. and Yavany Mt.–Sangachal, the crystalline basements occurs at 6 and 12 km, respectively.

The major part of the regional anomalies is caused by the topography of the pre-Mesozoic crystalline basement.

Acknowledgements

I would like to thank H. Karsli and N. Maden of the Black Sea Technical University, Turkey, for their support in the computing and in the preparation of the manuscript. I also thank M. Tagiyev of the Geology Institute of Azerbaijan for his assistance in the preparation of the English version of the manuscript.

References

Geological State Committee, Geology Institute, Azerbaijan Academy of Sciences, Agabekov, M.G., Azizbekov, Sh.A., Akhmedbeyli, F.S., Gadjiev, T.G., Grigoryants, B.V., Mamedov, A.V., Shikalibeyli, E.Sh., 1972. Tectonic scheme of Azerbaijan, 1:1,000,000. In: Azizbekov, Sh.A. (Ed.), Geology of the USSR, Azerbaijan vol. XLVII Nedra, Moscow, (in Russian).

Aksyonovich, G.I., Aronov, L.E., Galperin, E., Kosminskaya, I.P., Gegelgants, A.A., 1962. Deep Seismic Sounding in Central Part of the Caspian Sea. Publishing House of USSR Academy of Sciences, Moscow, (in Russian).

Azizbekov, Sh.A., Agabekov, M.G., Grigoryants, B.V., Shikalibeyli, E.Sh., Mamedov, A.V., 1972. The history of the geological evolution. In: Azizbekov, Sh.A. (Ed.), Geology of the USSR, Azerbaijan vol. XLVII Nedra, Moscow, pp. 441–503, (in Russian).

Bhaskara Rao, D., 1986. Modelling of sedimentary basins from gravity anomalies with variable density contrast. Geophys. J. R. Astron. Soc. 84 (1), 207–212.

Bhaskara Rao, D., Ramesh Babu, N., 1991. A fortran-77 computer program for three-dimensional analysis of gravity anomalies with variable density contrast. Comput. Geosci. 17, 655–667.

Bhattacharyya, B.K., 1966. Continuous spectrum of the total magnetic anomaly due to a rectangular prismatic body. Geophysics 31, 97–121.

Bracewell, R.N., 1983. Discrete Hartley transform. J. Opt. Soc. Am. 73, 1832–1835.

Bracewell, R.N., 1986. The Fourier Transform and Its Applications. McGraw-Hill Book Co., New York , 474 pp.

Gadjiyev, R.M., 1965. Deep Geologic Structure of Azerbaijan. Azerneshr, Baku, 205 pp. (in Russian).

Hartley, R.V.L., 1942. A more symmetrical Fourier analysis applied to transmission problems. Proc. IRE 30 (2), 144–150.

Kulhânek, O., 1976. Introduction to Digital Filtering in Geophysics. Elsevier, Amsterdam, 169 pp.

Mohan, N.L., Anand Babu, L., 1994. A note on 2D Hartley transform. Geophysics 59, 1150–1155.

Radjabov, M.M., 1978. Study of the structure of the earth's crust-consolidated complex of the Azerbaijan using deep seismic sounding and refracted wave-correlation method data. The Structure of the Earth's Crust and Upper Mantle in the Central and East Europe. Naukova Dumka, Kiev, pp. 205–211, (in Russian).

Rao, B.N., Rama, K.P., Markandeyulu, A., 1995. Mapros — a computer program for basement mapping and filtering of gravity and magnetic data using a Hartley transform. Comput. Geosci. 22, 197–218.

Saatcilar, R., Ergintav, S., Canitez, N., 1990. The use of the Hartley transform in geophysical applications. Geophysics 55, 1488–1495.

Shikhalibeyli, E.Sh., 1972. Location of Azerbaijan in general structure of the Caucasus and surrounding folded region. In: Azizbekov, Sh.A. (Ed.), Geology of the USSR, Azerbaijan vol. XLVII Nedra, Moscow, pp. 286–290, (in Russian).

Spector, A., Grant, F.S., 1970. Statistical models for interpreting aeromagnetic data. Geophysics 35, 293–302.

Sundararajan, N., 1995. 2-D Hartley transforms. Geophysics 60, 262–267.

Tsimmelzon, I.O., 1965. Geological interpretation of the local gravity anomalies of the Absheron peninsula and the Near-Caspian region. Explor. Min. Geophys. 38, 13–24, (in Russian).

Volarovich, M.P., Bayuk, E.I., Salekhli, T.M., Guseynov, F.G., 1966. Compressional wave velocities in sedimentary rocks of Azerbaijan under confining pressures to 4000 kg/cm^2. Transactions of Institute of the Earth's Physics vol. 37 Nauka, Moscow, pp. 130–139, (204, in Russian).